

Reactivity of Silylated Dinuclear Iron–Platinum Acyl Complexes: Formation of μ -Vinylidene Complexes and Crystal Structures of the Acyl Complex $[(OC)_3\{(MeO)_3Si\}Fe(\mu-dppm)Pt\{C(O)Me\}(t-BuNC)]$ and the μ -Vinylidene Complex $[(OC)_3Fe\{\mu-C=C(H)Ph\}(\mu-dppm)Pt(PPh_3)]$

Michael Knorr^{*,†} and Carsten Strohm[†]

*Universität des Saarlandes, Anorganische Chemie, Postfach 151150,
D-66041 Saarbrücken, Germany*

Pierre Braunstein[‡]

*Laboratoire de Chimie de Coordination, Associé au CNRS (URA 0416), Université Louis
Pasteur, 4 rue Blaise Pascal, F-67070 Strasbourg Cedex, France*

Received April 4, 1996[®]

Addition of RNC to the heterobimetallic acyl complex $[(OC)_3Fe\{\mu-Si(OMe)_2(OMe)\}(\mu-dppm)Pt\{C(O)Me\}]$ (**1a**), which displays a $\mu-\eta^2-Si-O$ bridge, afforded the isonitrile adducts $[(OC)_3\{(MeO)_3Si\}Fe(\mu-dppm)Pt\{C(O)Me\}(C\equiv NR)]$ (**3a** R = *t*-Bu, **3b** R = 2,6-xylyl). Upon treatment of a CH_2Cl_2 solution of **1a** with $MeO_2CC\equiv CCO_2Me$ (DMAD), alkyne insertion into the Pt–C bond gave the alkenyl complex $[(OC)_3Fe\{\mu-Si(OMe)_2(OMe)\}(\mu-dppm)Pt\{\mu-C=C(CO_2Me)C(O)Me\}]$ **4**. The isonitrile adducts $[(OC)_3\{(MeO)_3Si\}Fe(\mu-dppm)Pt\{\mu-C=C(O_2Me)C(O)Me\}(C\equiv NR)]$ (**5a** R = *t*-Bu, **5b** R = 2,6-xylyl) were isolated after addition of RNC. A more complex reaction occurred when phenylacetylene or *tert*-butylacetylene were reacted with **1a**. The iron-bound $Si(OMe)_3$ group and the organic ligand coordinated on platinum were eliminated, and the vinylidene-bridged complexes $[(OC)_3Fe\{\mu-C=C(H)R\}(\mu-dppm)Pt(CO)]$ (**6a** R = Ph, **6b** R = *t*-Bu, **6c** R = *n*-Bu) were obtained. The loosely Pt-bound CO ligand of **6a–c** was readily displaced by PPh_3 , $P(OMe)_3$, or 2,6-xylyl isonitrile yielding the substitution products $[(OC)_3Fe\{\mu-C=C(H)R\}(\mu-dppm)Pt(L)]$ (**7a** R = Ph, L = PPh_3 ; **7b** R = *t*-Bu, L = PPh_3 ; **7c** R = *t*-Bu, L = $P(OMe)_3$; **7d** R = *t*-Bu, L = 2,6-xylylNC). The heterobimetallic phenyl complex $[(OC)_3Fe\{\mu-Si(OMe)_2(OMe)\}(\mu-dppm)Pt(Ph)]$ (**8**) was obtained by reaction of $K[Fe\{Si(OMe)_3\}(CO)_3(\eta^1-dppm)]$ with a cold THF solution of $[PtCl(Ph)(1,5-COD)]$. The $\mu-\eta^2-Si-O$ bridge is readily opened under a CO atmosphere to give the CO adduct $[(OC)_3Fe\{Si(OMe)_3\}(\mu-dppm)Pt(CO)(Ph)]$ (**9**), which unexpectedly does not insert CO into the Pt–phenyl bond. This complex reversibly loses the CO ligand under reduced pressure to regenerate **8**. All complexes have been studied by multinuclear NMR spectroscopy. The solid state structures of complexes **3a** and **7a** have been determined by single-crystal X-ray diffraction.

Introduction

We reported recently on mechanistic aspects of the facile migratory insertion of CO into the Pt–C bond of heterodinuclear alkyl complexes leading to the stable acyl complexes $[(OC)_3Fe\{\mu-Si(OMe)_2(OMe)\}(\mu-dppm)Pt\{C(O)R\}]$ (R = Me, Et, norbornyl).^{1,2,6} In a similar manner we obtained also the palladium analogue $[(OC)_3Fe\{\mu-Si(OMe)_2(OMe)\}(\mu-dppm)Pd\{C(O)Me\}]$ **1b**, which

is prone to further insertion of strained olefins.^{3–6} We were interested in probing the possibility to insert other small molecules into the M–C bond to form longer organic chains and to study the influence of two different adjacent metals on the reactivity of the metal-carbon bond compared to that in mononuclear alkyl and acyl compounds. The main emphasis of this paper concerns the insertion of alkynes in the Pt–acyl bond of $[(OC)_3Fe-$

(3) Braunstein, P.; Knorr, M. *J. Organomet. Chem.* **1995**, *500*, 21.

(4) (a) Braunstein, P.; Knorr, M. In *Organosilicon Chemistry II*; Auner, N., Weis, J., Eds.; VCH: Weinheim (Germany), 1996; p. 553. (b) Braunstein, P.; Knorr, M. In *Metal-Ligand Interactions, Structure and Reactivity*; NATO ASI Series; Russo, N., Salahub, D. R., Eds.; Kluwer Academic Publishers: Dordrecht, The Netherlands, 1996; p. 49.

(5) Braunstein, P.; Knorr, M.; Stährfeldt, T. *J. Chem. Soc., Chem. Commun.* **1994**, 1913.

(6) Braunstein, P.; Faure, T.; Knorr, M.; Stährfeldt, T.; DeCian, A.; Fischer, J. *Gazz. Chim. Ital.* **1995**, *125*, 35.

[†] E-mail: m.knorr@sbusol.rz.uni-sb.de.

[‡] E-mail: braunst@chimie.u-strasbg.fr.

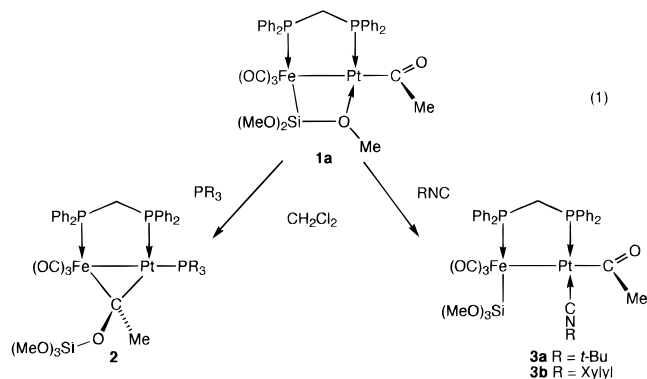
[®] Abstract published in *Advance ACS Abstracts*, November 1, 1996. (1) Knorr, M.; Braunstein, P.; Tiripicchio, A.; Ugozzoli, F. *Organometallics* **1995**, *14*, 4910.

(2) Knorr, M.; Braunstein, P.; DeCian, A.; Fischer, J. *Organometallics* **1995**, *14*, 1302.

$\{\mu\text{-Si}(\text{OMe})_2(\text{OMe})\}(\mu\text{-dppm})\text{Pt}\{\text{C}(\text{O})\text{Me}\}$ **1a** and the subsequent formation of heterobimetallic μ -vinylidene complexes, which were thoroughly studied by multinuclear NMR spectroscopy and X-ray diffraction.

Results and Discussion

Whereas addition of PR_3 to the acyl complex **1a** induced a silyl shift of the $\text{Si}(\text{OMe})_3$ group onto the oxygen atom of the acyl ligand and afforded $[(\text{OC})_3\text{Fe}\{\mu\text{-C}(\text{R})\text{OSi}(\text{OMe})_3\}(\mu\text{-dppm})\text{Pt}(\text{PR}_3)]$ **2** with a μ -siloxycarbene ligand, addition of *t*-BuNC gave exclusively the isonitrile adduct $[(\text{OC})_3\{\text{MeO}\}_3\text{Si}\{\text{Fe}(\mu\text{-dppm})\text{Pt}\{\text{C}(\text{O})\text{Me}\}(t\text{-BuNC})\}]$ **3a**, which has already been briefly mentioned.^{2,6} Since aromatic isonitriles are known to insert more readily into M–C bonds due to their more electrophilic character, we reacted **1a** with 2,6-xylyl isonitrile. Again, no insertion into the Pt–C bond took place even in the presence of excess isocyanide. Instead of the hoped for insertion product, the derivative $[(\text{OC})_3\{\text{MeO}\}_3\text{Si}\{\text{Fe}(\mu\text{-dppm})\text{Pt}\{\text{C}(\text{O})\text{Me}\}(2,6\text{-xylylNC})\}]$ **3b** was isolated in the form of yellow crystals, which are air-stable for short periods of time. Even after several days in solution **3b** showed no tendency to rearrange. In contrast to the very sharp lines in the ²⁹Si- and ³¹P-NMR spectra, the doublet resonance with a ¹J(P–Pt) coupling of 3595 Hz in the ¹⁹⁵Pt NMR spectrum of **3b** was very broad. This may perhaps be due to a rapid isonitrile dissociation/association process associated with closing and opening of the $\mu\text{-}\eta^2\text{-Si-O}$ bridge, respectively. This could explain why in the ¹³C{¹H} NMR of **3b** recorded at ambient temperature no resonance for the isonitrile carbon could be detected despite an extended data acquisition time and good signal to noise ratio.



Crystal Structure of 3a. Since available structural data for Pt–acyl complexes appear to be limited to mononuclear complexes,^{7–11} we performed a crystal structure determination on **3a**. Views of the structure of **3a** are shown in Figures 1 and 2; selected bond distances and angles are listed in Table 1. The Fe and Pt moieties are linked by a single dppm bridge to give

Table 1. Selected Bond Distances (Å) and Angles (deg) for Complex **3a**

Fe–Si	2.296(3)	Pt–Fe–Si	94.77(7)
Pt–Fe	2.798(2)	C(9)–Pt–C(7)	84.5(3)
Pt–C(9)	1.989(8)	P(1)–Fe–Pt	92.33(7)
Pt–C(7)	2.056(8)	P(2)–Pt–Fe	92.77(6)
Fe–P(1)	2.224(3)	P(2)–Pt–C(7)	86.3(2)
Pt–P(2)	2.273(3)	P(2)–Pt–C(9)	164.5(2)
Fe–C(1)	1.745(7)	C(9)–Pt–Fe	98.0(2)
Fe–C(2)	1.770(8)	C(7)–Pt–Fe	172.1(2)
Fe–C(3)	1.764(7)	C(1)–Fe–C(3)	105.9(3)
Si–O(4)	1.642(6)	C(1)–Fe–C(2)	112.1(3)
Si–O(5)	1.646(5)	C(3)–Fe–C(2)	140.1(3)
Si–O(6)	1.641(5)	P(1)–Fe–Si	171.62(8)
N–C(9)	1.132(9)	P(1)–C(26)–P(2)	112.4(3)
N–C(10)	1.444(10)	N–C(9)–Pt	171.1(8)
O(1)–C(1)	1.159(8)	C(9)–N–C(10)	169.7(9)
O(2)–C(2)	1.155(8)	O(7)–C(7)–C(8)	121.6(8)
O(3)–C(3)	1.160(8)	O(7)–C(7)–Pt	124.3(7)
O(7)–C(7)	1.175(10)		
C(7)–C(8)	1.514(13)		

a five-membered Fe–P(1)–C(26)–P(2)–Pt ring. The Fe–Pt distance of 2.798(2) Å indicates a metal–metal bond, and the Fe–P(1) and Pt–P(2) distances are of 2.224(3) and 2.273(3) Å, respectively. These distances lie in the range found in similar complexes. The environment of the Fe atom is determined by the Pt atom, a phosphorus atom from the dppm ligand, a Si atom from the $\text{Si}(\text{OMe})_3$ group, and by three carbon atoms from terminal, meridional arranged carbonyl ligands. The $\text{Si}(\text{OMe})_3$ ligand is trans to the P(1) atom (P(1)–Fe–Si 171.62(8)°). Two linear CO ligands (175.9(7)° for Fe–C(2)–O(2) and 173.4(7)° for Fe–C(3)–O(3)) are leaning toward the adjacent metal rather than semibridging. The Pt–C(2) and Pt–C(3) distances of 2.818 and 2.727 Å, respectively, appear indeed too long to represent a significant bonding interaction and are longer than the 2.211(8) Å found for a semibridging CO.¹² The C–Fe–C angles are in the range 105.9(3)–140.1(3)°, intermediate between the values expected for an octahedral or a trigonal bipyramidal Fe coordination. The geometry around the Fe atom can be viewed as distorted octahedral, consistent with a formal Fe(d⁷)–Pt(d⁹) situation, or alternatively as distorted trigonal bipyramidal, corresponding to a formal dative Fe(d⁸) → Pt(d⁸) interaction. This ligand arrangement has been observed in most heterobimetallic complexes containing a Fe(SiR₃)(CO)₃(PR₃) moiety.^{6,13}

The geometry around the platinum atom is approximately square planar. The metal bound C(7) acyl carbon is almost colinear with the Fe–Pt axis forming a C(7)–Pt–Fe angle of 172.1(2)° and orthogonal to the P(2) atom with a C(7)–Pt–P(2) angle of 86.3(2)°. The distance Pt–C(7) of 2.056(8) Å is intermediate between the values of 1.974(9) Å reported for [Pt{C(O)Me}(bzac)(PPh₃)] (bzac = 3-mercapto-1-phenylbut-2-en-1-onate)⁹ and the 2.08(2) Å found for *trans*-[Pt(I){C(O)C=CMe₂}(PPh₃)₂].¹⁰ Probably for steric reasons, the isonitrile ligand deviates from the P(1)–Fe–Pt–P(2) plane to minimize the repulsion with the $\text{Si}(\text{OMe})_3$ moiety (C(9)–O(5) = 2.9 Å): the C(9)–Pt–P(2) angle is 164.5(2)° and the torsion angle Si–Fe–Pt–C(9) is 30.5(3)° (Figure 2). The three methyl carbons C(11)–C(13) of the *t*-BuNC ligand are disordered (see Experimental Section). The

(7) Bardi, R.; Piazzesi, A. M.; Cavinato, G.; Cavoli, P.; Toniolo, T. *J. Organomet. Chem.* **1982**, *224*, 407.

(8) Sen, A.; Chen, J. T.; Vetter, W. M.; Whittle, R. R. *J. Am. Chem. Soc.* **1987**, *109*, 148.

(9) Cavell, K. J.; Jin, H.; Skelton, B. W.; White, A. W. *J. Chem. Soc., Dalton Trans.* **1992**, 2923.

(10) Stang, P. J.; Zhong, Z.; Arif, A. M. *Organometallics* **1992**, *11*, 1017.

(11) Chen, J. T.; Yeh, Y. S.; Yang, C. S.; Tsai, F. Y.; Huang, G. L.; Shu, B. C.; Huang, T. M.; Chen, Y. S.; Lee, G. H.; Cheng, M. C.; Wang, C. C.; Wang, Y. *Organometallics* **1994**, *13*, 4804.

(12) Jacobsen, G. B.; Shaw, B. L.; Thornton-Pett, M. *J. Chem. Soc., Dalton Trans.* **1987**, 3079.

(13) Braunstein, P.; Faure, T.; Knorr, M.; Balegroune, F.; Grandjean, D. *J. Organomet. Chem.* **1993**, *462*, 271.

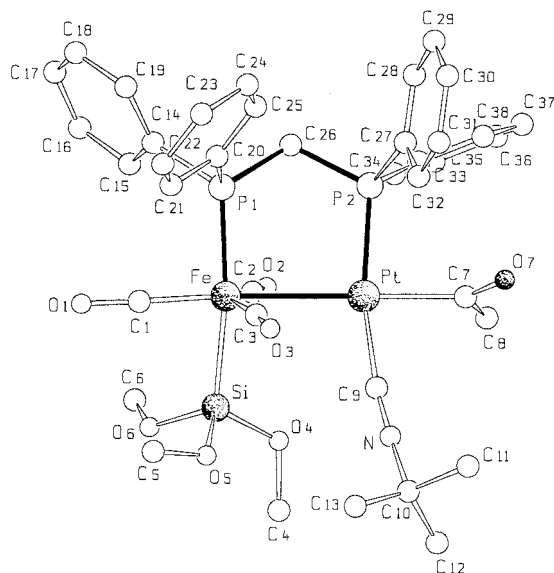


Figure 1. View of the structure of $[(OC)_3\{(MeO)_3Si\}Fe(\mu\text{-dppm})Pt\{C(O)Me\}(t\text{-BuNC})]$ **3a** in the crystal with the atom numbering scheme.

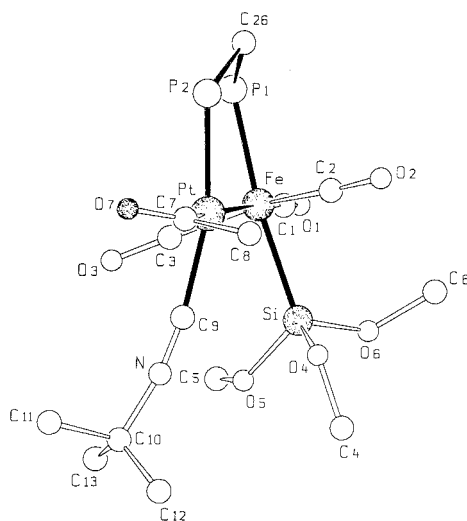
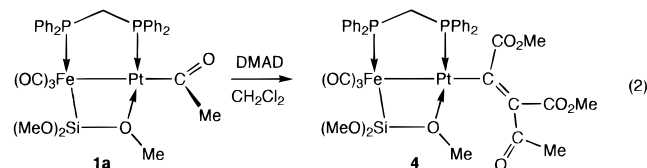


Figure 2. Perspective view of the core structure of $[(OC)_3\{(MeO)_3Si\}Fe(\mu\text{-dppm})Pt\{C(O)Me\}(t\text{-BuNC})]$ **3a** along the Fe–Pt axis. The phenyl groups are omitted for better clarity.

C(9)–Pt–Fe and Si–Fe–Pt angles of $98.0(2)^\circ$ and $94.77(7)^\circ$, respectively, also reflect the steric hindrance between the silyl and isonitrile ligand. As found in the mononuclear Pt–acyl complexes mentioned above and in related Pd–acyl complexes,^{14,15} the acyl plane Pt–C(7)–O(7) is roughly perpendicular to the P(1)–Fe–Pt–P(2) mean plane with a dihedral angle of $70.7(7)^\circ$. The torsion angle P(2)–Pt–C(7)–O(7) is $77.5(8)^\circ$. The Pt–C(9) distance of $1.989(8)$ Å is somewhat elongated compared to those usually found for terminal Pt–CN*t*-Bu distances as for example in the cluster $[Pt_3(t\text{-BuNC})_6]$ ($1.90(2)$ Å)¹⁶ but is similar to that in $[(OC)_3\{(MeO)_3Si\}Fe(\mu\text{-dppm})HgPt(C_6Cl_5)(t\text{-BuNC})]$ ($1.99(3)$ Å).¹⁷

DMAD Insertion. In contrast to the adduct formation with the isonitrile ligands described above, the

activated alkyne $MeO_2CC\equiv CCO_2Me$ (DMAD) readily inserted under mild conditions into the Pt–acyl bond of **1a** to afford the yellow alkenyl complex $[(OC)_3Fe\{\mu\text{-Si}(OMe)_2(OMe)\}(\mu\text{-dppm})Pt\{(MeO_2C)C=C(CO_2Me)C(O)Me\}]$ **4**.



Its ^{31}P -NMR spectrum exhibits a doublet at δ 55.3 for the dppm phosphorus on iron and a doublet at δ 2.1 for the Pt–bound phosphorus, whose $^{2+3}J(P\text{-}P)$ coupling of 43 Hz is diagnostic for the conservation of the four-

membered $FeSiO\rightarrow Pt$. The $^1J(Pt\text{-}P)$ and $^{2+3}J(Pt\text{-}P)$ couplings of 4812 and 44 Hz are also found in the ^{195}Pt -NMR spectrum, which displays a doublet of doublets centered at δ –2224 ppm. In the proton NMR spectrum the observation of two different signals for the SiOMe groups at δ 3.83 and 3.78 in a 1:2 ratio, two singlets for the C(O)OMe groups at δ 3.52 and 3.44 and an acyl resonance at δ 1.97 corroborates our structural proposal for **4**. We also tried to insert $PhC\equiv CMe$ into the Pt–acyl bond. However, even in the presence of a tenfold excess of $PhC\equiv CMe$ and gentle heating in CH_2Cl_2 no reaction occurred and **1a** was recovered unchanged. This is in agreement with the early results of Clark *et al.* on alkyne insertion into the Pt–Me bond of mononuclear complexes.¹⁸ Whereas alkynes with electron-withdrawing groups such as DMAD or hexafluorobutyne inserted readily to give vinyl complexes, $PhC\equiv CMe$ or $PhC\equiv CPh$ were inert toward insertion into the Pt–Me bond. In the case of **1a**, two mechanistic possibilities are conceivable for the DMAD insertion: (i) the insertion could be initiated by the formation of a five-coordinated transition state or intermediate with the alkyne bound in direction of the dz^2 orbital of the platinum center, or (ii) the insertion could be facilitated by an opening of the $\mu\text{-Si-O}$ bridge and liberation of a vacant coordination site, which would then be occupied by the alkyne. Theoretical studies, which have been experimentally confirmed, on the insertion of alkynes in Pd–acyl complexes,¹⁹ predict a reaction mechanism involving a four-center transition state.²⁰ Since we have no spectroscopic evidence for intermediates as in the case of the CO insertion,⁶ we cannot comment further on which mechanism is operating.

The $\mu\text{-Si-O}$ bridge opens instantaneously upon addition of isonitrile to a CH_2Cl_2 solution of **4** to give the stable adducts $[(OC)_3\{(MeO)_3Si\}Fe(\mu\text{-dppm})Pt\{(MeO_2C)C=C(CO_2Me)C(O)Me\}(CNR)]$ (**5a**, R = *t*-Bu; **5b**, R = 2,6-xylyl), which were fully characterized by elemental analysis, mass spectroscopy, and IR and NMR spectroscopy. As in the case of **3b** no resonance for the isonitrile carbon could be detected in the $^{13}C\{^1H\}$ NMR

(14) Markies, B. A.; Wijkens, P.; Boersma, J.; Spek, A. L.; van Koten, G. *Recl. Trav. Chim. Pays-Bas* **1991**, *110*, 133.

(15) Markies, B. A.; Kruijs, D.; Rietveld, M. H. P.; Verkerk, K. A. N.; Boersma, J.; Kooijman, H.; Lakin, M. T.; Spek, A. L.; van Koten, G. *J. Am. Chem. Soc.* **1995**, *117*, 5263.

(16) Green, M.; Howard, J. A. K.; Murray, M.; Spencer, J. L.; Stone, F. G. A. *J. Chem. Soc., Dalton Trans.* **1977**, 1509.

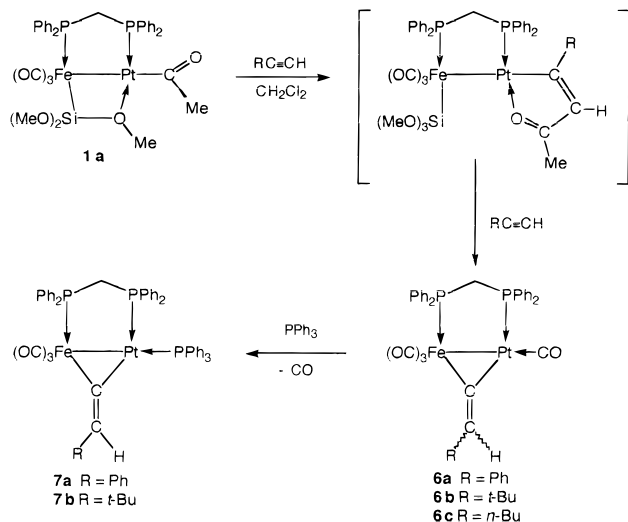
(17) Braunstein, P.; Knorr, M.; Strampfer, M.; Tiripicchio, A.; Ugozzoli, F. *Organometallics* **1994**, *13*, 3038.

(18) (a) Clark, H. C.; Jablonski, C. R.; von Werner, K. *J. Organomet. Chem.* **1974**, *82*, C51. (b) Clark, H. C.; von Werner, K. *J. Organomet. Chem.* **1975**, *101*, 347.

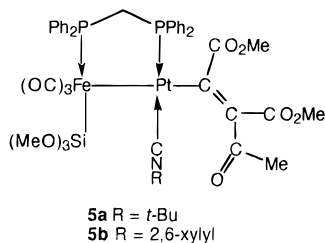
(19) Samsel, E. G.; Norton, J. R. *J. Am. Chem. Soc.* **1984**, *106*, 5505.

(20) Thorn, D. L.; Hoffmann, R. *J. Am. Chem. Soc.* **1978**, *100*, 2079.

Scheme 1



spectrum of **5a** in spite of an extended data acquisition time. Although isonitrile insertion reactions into Pt–alkenyl bonds of mononuclear complexes are known,²¹ samples of **5** were recovered unchanged after 24 h in CH₂Cl₂ solution.



Formation of μ -Vinylidene Complexes. When **1a** was reacted with a tenfold excess of phenylacetylene a more complex reaction occurred which led after 24 h to the vinylidene-bridged complex [(OC)₃Fe{ μ -C=C(H)Ph}-(μ -dppm)Pt(CO)] **6a** (Scheme 1). This complex was isolated in ca. 59% yield as a brown waxy solid, which was difficult to purify from excess of phenylacetylene and other organic silylated byproducts and traces of other uncharacterized organometallic complexes. After extraction of the crude material with diethyl ether, pure **6a** was isolated as an orange brown powder. Similar transformations occur with the more reactive *tert*-butylacetylene to yield the stable vinylidene-bridged final product [(OC)₃Fe{ μ -C=C(H)*t*-Bu}-(μ -dppm)Pt(CO)] **6b**. Compared to the reaction with HC≡CPh, the rate of this transformation is significantly enhanced. ³¹P NMR monitoring revealed that after 4 h all **1a** had been consumed, affording **6b** as the major species (ca. 85–90% by spectral integration). The formation of [(OC)₃Fe{ μ -C=C(H)*n*-Bu}-(μ -dppm)Pt(CO)] **6c** could be observed spectroscopically after treatment of **1a** with 1-hexyne.

Spectroscopic Studies. The structure of complexes **6** could be unambiguously deduced from the combined NMR and IR data as exemplified below for **6a**. The ³¹P-{¹H} NMR data of **6a** are very different from those of the alkenyl complex **4** and resemble those of the previously described μ -carbene complexes [(OC)₃Fe{ μ -

C(Et)OSi(OMe)₃}(μ -dppm)Pt(C≡NR)].² They consist of a doublet at δ 60.8 with a ²⁺³*J*(P–P) coupling of 125 Hz and further ²⁺³*J*(Pt–P) coupling of 80 Hz for the Fe-bound phosphorus and a second doublet at δ 21.9 with a ¹*J*(Pt–P) coupling of 2368 Hz. These Pt–P couplings are also found in the ¹⁹⁵Pt{¹H} NMR spectrum which displays a doublet of doublets at δ –2336. In the ¹H NMR spectrum a triplet due to the dppm protons is found at δ 4.17 (²*J*(P–H) = 10.2 Hz), which displays an additional ³*J*(Pt–H) coupling of 41.6 Hz. Apart from the phenyl resonances in the range between 6.70–7.75 ppm, only one other resonance was detected at δ 8.65. We assign this doublet of doublets with couplings of 9.5 and 18.3 Hz to the proton of the μ -C=C(H)Ph ligand. Similar chemical shifts and couplings have been reported by Antonova *et al.* for phenylethenylidene-bridged heterobimetallics of the type [(OC)₂CpMn{ μ -C=C(H)Ph}Pt(PR₃)₂]^{22,23} and by Lukehart for the cationic complex [(OC)CpFe(μ -CO){ μ -C=C(H)Ph}Pt(PEt₃)₂][PF₆].²⁴ The ¹³C{¹H} NMR spectrum recorded at ambient temperature displayed broad resonances in the carbonyl region and in the range expected for the α -vinylidene carbon atom. More informative was the spectrum recorded at 253 K. A sharp doublet of doublets for the α -vinylidene carbon atom with ²*J*(P–C) couplings of 11 and 58 Hz was now observed at δ 238.5. A similar chemical shift has been reported by Werner *et al.* for the phenylvinylidene-bridged complex [(OC)₃Fe(μ -CO){ μ -C=C(H)Ph}RhCp(PⁱPr₃)].²⁵ A broad singlet at δ 143.9 (with a ²*J*(Pt–C) coupling of 114 Hz) arises from the β -vinylidene carbon atom. For the Fe–Rh complex cited above a β -vinylidene carbon resonance was found at δ 140.0.²⁵ The presence of three CO ligands coordinated on iron is indicated by a broad singlet at δ 215.9 and a doublet at δ 212.6 in a 1:2 intensity ratio. The Pt–bound CO ligand was detected at δ 188.7. The IR spectrum of **6a** in the ν (CO) region shows an appearance and a position of the ν (CO) vibrations (2011(s) and 1953(vs) cm^{–1}) which are very reminiscent of the IR spectrum of the siloxycarbene complex [(OC)₃Fe{ μ -C(Me)OSi(OSiMe)₃}(μ -dppm)Pd(CO)].¹ The Pt–bound CO gives rise to an absorption at 2021 cm^{–1}. A weak band at 1591 cm^{–1} is probably due to the ν (C=C) vibration of the vinylidene unit. The spectroscopic data of **6b** are given in the Experimental Section.

The strong electron-withdrawing property and close electronic relationship between vinylidene and aminocarbyne ligands has been confirmed both experimentally²³ and theoretically by molecular orbital calculations.²⁶ A related heterobimetallic W–Pt μ -vinylidene complex has been prepared by deprotonation of the alkylidyne bridged complex [(OC)Pt(μ -dppm)(μ -CMe)W(CO)₄][BF₄] with K[BH(CHMeEt)₃] to give [(OC)Pt(μ -dppm)(μ -C=CH₂)W(CO)₄] which possesses a ligand arrangement very similar to that in **6**.²⁷

(22) Antonova, A. B.; Kovalenko, S. V.; Korniyets, E. D.; Petrovsky, P. V.; Gulbis, G. R.; Johansson, A. A. *Inorg. Chim. Acta* **1985**, *96*, 1.

(23) Antonova, A. B.; Kovalenko, S. V.; Korniyets, E. D.; Petrovsky, P. V.; Johansson, A. A.; Deykhina, N. A. *Inorg. Chim. Acta* **1985**, *105*, 153.

(24) Afzal, D.; Lukehart, C. M. *Organometallics* **1987**, *6*, 546.

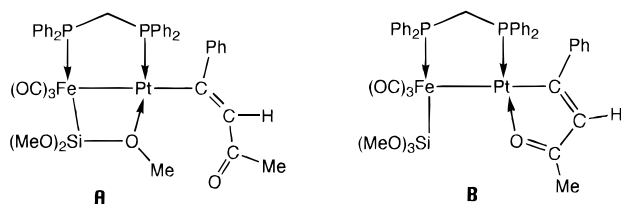
(25) Werner, H.; Alonso, F. J. G.; Otto, H.; Peters, K.; von Schnering, H. G. *Chem. Ber.* **1988**, *121*, 1565.

(26) Kostic, N. M.; Fenske, R. F. *Organometallics* **1982**, *1*, 974.

(27) Awang, M. R.; Jeffery, J. C.; Stone, F. G. A. *J. Chem. Soc., Dalton Trans.* **1983**, 2091.

(21) (a) Otsuka, S.; Ataka, K., *J. Chem., Dalton Trans.* **1976**, 327.
(b) Wouters, J. M. A.; Klein, R. A.; Elsevier, C. J.; Zoutberg, M. C.; Stam, C. H. *Organometallics* **1993**, *12*, 3864.

On monitoring the course of the reaction by ^{31}P NMR and ^{13}C spectroscopy the formation of an intermediate was observed ca. 40 min after addition of a tenfold excess of phenylacetylene to a solution of **1a** in CDCl_3 . This new species displays in the $^{31}\text{P}\{^1\text{H}\}$ NMR spectrum an AX pattern ($^{2+3}J(\text{P}-\text{P}) = 53$ Hz) with doublets at δ 50.1 and 4.2, which are flanked by platinum satellites with couplings of 51 and 2262 Hz, respectively. The concentration of **1a** and the intermediate decreases gradually while that of **6a** increases. After 24 h, **1a** and the intermediate have been consumed and **6a** remains as the only detectable species, together with traces (less than 10%) of other unknown compounds. We suggest that this complex reaction leading to **6a** is initiated by insertion of phenylacetylene into the platinum–acyl bond of **1a** to give the observed intermediate, whose possible structures are proposed below.



Intermediate **A** with the acyl group bound to the less sterically hindered alkyne carbon would correspond to the DMAD-insertion product **4**. However, the different $J(\text{P}-\text{P})$ coupling and in particular the $^1J(\text{Pt}-\text{P})$ couplings (2262 vs 4812 Hz) are in marked contrast. We are in favor of a formulation of type **B** with a ketonic interaction of the former acyl oxygen with the platinum center, although it is not clear why the $^1J(\text{Pt}-\text{P})$ coupling constant should be so sensitive to the nature of the oxygen donor atom trans to phosphorus. This suggestion is also corroborated by ^{13}C -NMR monitoring of the reaction of phenylacetylene with **1a**, which was ^{13}C labeled on the acyl group. The acyl resonance (99% enriched) of **1a** at δ 233.5 decreases and a new broadened resonance emerges at δ 227.0. After ca. 3 h this resonance represents the most intense signal. In addition to unreacted **1a**, the Pt–bound CO-resonance of **6a** and a sharp new singlet at δ 197.6 are detected in the carbonyl region. Closely related complexes have been isolated upon treatment of $[(\text{OC})_3\text{Fe}\{\mu\text{-Si}(\text{OMe})_2(\text{OMe})\}(\mu\text{-dppm})\text{Pd}\{\text{C}(\text{O})\text{Me}\}]$ **1b** with norbornene and norbornadiene.⁵ Since the norbornadiene insertion product $[(\text{OC})_3\{\mu\text{-Si}(\text{OMe})_2(\text{OMe})\}\text{Fe}(\mu\text{-dppm})\text{Pd}\{\text{C}_7\text{H}_8\text{C}(\text{=O})\text{Me}\}]$ displays the resonance for the ketonic carbonyl group at δ 228.8, we attribute the resonance at δ 227.0 to the ketonic carbonyl group of intermediate **B**.

A related ketonic interaction resulting in a five-membered ring has also been observed by Carmona *et al.* upon insertion of $\text{PhC}\equiv\text{CH}$ into the Ni–C(O)R bond of *trans*- $[\text{NiCl}\{\text{C}(\text{O})\text{CH}_2\text{SiMe}_3\}(\text{PMe}_3)_2]$. The structure of the insertion product *trans*- $[\text{NiCl}\{\text{C}(\text{Ph})=\text{C}(\text{H})\text{C}(\text{O})\text{CH}_2\text{SiMe}_3\}(\text{PMe}_3)_2]$ was ascertained by an X-ray diffraction study.²⁸ Similar metallacyclic alkenyl ketone

complexes have been obtained after phenylacetylene insertion in molybdenum– and tungsten–acyl bonds.²⁹

To account for the cleavage of the Fe–SiR₃ and the Pt–alkenyl bonds, we assume a sequence of several oxidative additions of $\text{RC}\equiv\text{CH}$ onto the platinum center followed by reductive elimination steps finally leading to **6**. A possible source for the new CO ligand could be the acyl group or decomposition of a $\text{Fe}(\text{CO})_3$ unit. We are in favor of the first possibility, since the high spectroscopic yield and the absence of insoluble materials during the NMR monitoring of the reaction (see above) are not consistent with a significant decomposition. Furthermore the NMR experiment with ^{13}C labeled **1a** demonstrates that the acyl group is the source of the platinum-bound carbonyl ligand. The silyl group may be lost as $\text{HSi}(\text{OMe})_3$ or in the form of the hydrosilation product $\text{Ph}(\text{H})\text{C}=\text{C}(\text{H})\text{Si}(\text{OMe})_3$.³⁰ Future GC/MS studies will be necessary to characterize the cleavage products in order to gain a better insight into the various mechanistic steps of this complex transformation.

Reactivity of 6 toward Nucleophiles. The Pt-bound CO ligand of **6a** can be readily substituted upon addition of PPh_3 to afford the very stable yellow vinylidene complex **7a** (Scheme 1). This complex has been fully analyzed by elemental analyses, multinuclear NMR investigations, IR spectroscopy, and X-ray diffraction. The coordination of the PPh_3 ligand can be deduced from the $^{31}\text{P}\{^1\text{H}\}$ -NMR spectrum, which shows a doublet of doublets at δ 63.4 for the iron-bound phosphorus atom, which is strongly coupled ($^{2+3}J(\text{P}-\text{P}) = 116$ Hz) with the platinum-bound dppm phosphorus, which resonates at δ 21.9. This signal is further split owing to the presence of the PPh_3 ligand which appears at δ 43.3 as a doublet of doublets with a typical *cis*-coupling of 18 Hz and a $^3J(\text{P}-\text{P})$ coupling of 14 Hz. The ^{195}Pt -NMR spectrum contains of a ddd resonance at -2695 ppm with a $^1J(\text{Pt}-\text{P})$ coupling of 2473 Hz with the dppm phosphorus, a further $^1J(\text{Pt}-\text{P})$ coupling of 4022 Hz with the PPh_3 ligand, and a $^{2+3}J(\text{Pt}-\text{P})$ coupling of 79 Hz. In the $^{13}\text{C}\{^1\text{H}\}$ -NMR spectrum of **7a** recorded at ambient temperature the Fe carbonyls give rise to a broad signal at δ 217.5. This fluxional behavior is frozen at 253 K, since two distinct signals at δ 218.2 (doublet) and 215.3 (doublet of doublets) are observed for the inequivalent Fe carbonyls in a 1:2 ratio. The μ - α -vinylidene carbon appears as a doublet of doublets centered at δ 236.9 with $^2J(\text{P}-\text{C})$ couplings of 10 and 70 Hz. The β -vinylidene carbon is detected at δ 141.1 as a broadened signal due to unresolved P–C couplings. Noteworthy are the unusually large long-range $^4J(\text{P}-\text{H})$ couplings observed in the ^1H NMR spectrum for the vinylidene proton situated at δ 6.32 with values of 34.6 Hz for **7a** and 27.8 Hz for **7b**. These couplings exceed even the $^4J(\text{P}-\text{H})$ couplings of 22.3 Hz quoted for $[(\text{OC})_2\text{-CpMn}\{\mu\text{-C}=\text{C}(\text{H})\text{Ph}\}\text{Pt}\{\text{P}(\text{OPh})_3\}_2]$ ²³ and of 26.3 Hz for $[(\text{OC})(\text{C}_6\text{F}_5)_2\text{Pt}\{\mu\text{-C}=\text{C}(\text{H})\text{Ph}\}\text{Pt}(\text{PPh}_3)_2]$.³¹ We explain the magnitude of these $^4J(\text{P}-\text{H})$ couplings by the *trans*-arrangement of the dppm backbone relative to the vinylidene bridge (see X-ray structure below).

(29) (a) Alt, H. G.; Engelhardt, H. E.; Thewalt, U.; Riede, J. *J. Organomet. Chem.* **1985**, *288*, 165. (b) Burkhardt, E. R.; Doney, J. J.; Bergman, R. G.; Heathcock, C. H. *J. Am. Chem. Soc.* **1987**, *109*, 2022.

(30) Adams, R. D.; Cortopassi, J. E.; Pompeo, M. P. *Organometallics* **1992**, *11*, 1.

(31) Ara, I.; Berenguer, J. R.; Fornies, J.; Lalinde, E.; Tomas, M. *Organometallics* **1996**, *15*, 1014.

(28) (a) Carmona, E.; Gutierrez-Puebla, E.; Monge, A.; Marin, J. M.; Paneque, M.; Poveda, M. L. *Organometallics* **1984**, *3*, 1438. (b) Carmona, E.; Gutierrez-Puebla, E.; Monge, A.; Marin, J. M.; Paneque, M.; Poveda, M. L. *Organometallics* **1989**, *8*, 967.

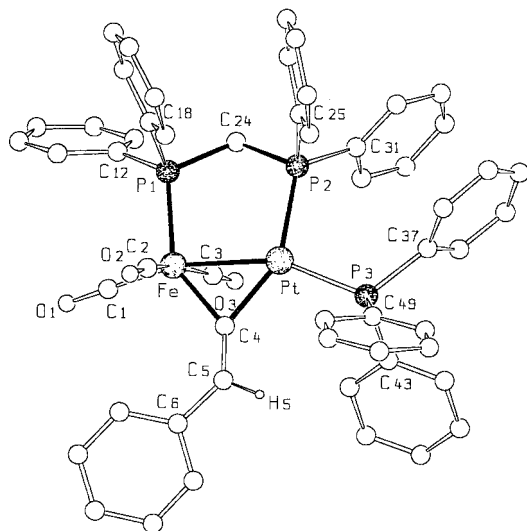
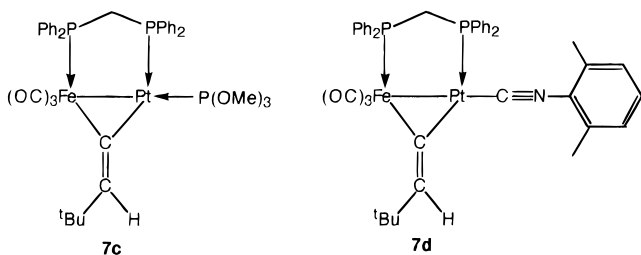


Figure 3. View of the structure of $[(\text{CO})_3\text{Fe}\{\mu\text{-C}=\text{C}(\text{H})\text{Ph}\}(\mu\text{-dppm})\text{Pt}(\text{PPh}_3)]$ **7a** in the crystal with the numbering scheme.

The very stable derivative $[(\text{OC})_3\text{Fe}\{\mu\text{-C}=\text{C}(\text{H})t\text{-Bu}\}(\mu\text{-dppm})\text{Pt}(\text{PPh}_3)]$ **7b**, whose spectroscopic data are given in the Experimental Section, was isolated upon addition of PPh_3 to a CH_2Cl_2 solution of **6b** in form of yellow crystals. In a similar manner the phosphite-substituted derivative $[(\text{OC})_3\text{Fe}\{\mu\text{-C}=\text{C}(\text{H})t\text{-Bu}\}(\mu\text{-dppm})\text{Pt}\{\text{P}(\text{OMe})_3\}]$ **7c** was prepared and spectroscopically investigated. Even with 2,6-xylylisonitrile the Pt-bound carbonyl is instantaneously displaced to give $[(\text{OC})_3\text{Fe}\{\mu\text{-C}=\text{C}(\text{H})t\text{-Bu}\}(\mu\text{-dppm})\text{Pt}(\text{C}\equiv\text{N-xylyl})]$ **7d**. This complex, which is closely related with its μ -siloxycarbene congener $[(\text{OC})_3\text{Fe}\{\mu\text{-C}(\text{Et})\text{OSi}(\text{OMe})_3\}(\mu\text{-dppm})\text{Pt}(\text{C}\equiv\text{N-xylyl})]$,² has been fully characterized by elemental analyses and multinuclear NMR spectroscopy. Owing to fluxional behavior, no resolved carbonyl and α -vinylidene signals could be detected in the $^{13}\text{C}\{^1\text{H}\}$ -NMR spectra of **7c** and **7d** recorded at 295 K. This dynamic behavior (carbonyl scrambling?) was sufficiently slowed down at 253 K, and well resolved signals were obtained for **7d** at δ 226.5 (dd, α -C), 217.6, and 215.3 (FeCO). In an NMR tube experiment we tried also to prepare **7d** by reacting **7b** with a large excess of *tert*-butylacetylene. However, after two days only unchanged $[(\text{OC})_3\{\text{MeO}\}_3\text{Si}\{\mu\text{-C}(\text{R})\text{OSi}(\text{OMe})_3\}(\mu\text{-dppm})\text{Pt}(\text{C}(\text{O})\text{Me})\{2,6\text{-xylyl}\}\text{NC}]$ **3b** was observed as the sole species.



Crystal Structure of $[(\text{CO})_3\text{Fe}\{\mu\text{-C}=\text{C}(\text{H})\text{Ph}\}(\mu\text{-dppm})\text{Pt}(\text{PPh}_3)]$ (7a**).** Crystals of **7a** containing 0.5 CH_2Cl_2 were grown from CH_2Cl_2 /hexane. A view of the structure is shown in Figure 3, and selected bond distances and angles are given in Table 2. The Fe–Pt distance of 2.5503(8) Å indicates a metal–metal bond and is close to the values found in other complexes of

Table 2. Selected Bond Distances (Å) and Angles (deg) for Complex **7a**

Pt–Fe	2.5503(8)	Fe–Pt–C(4)	50.3 (2)
Pt–C(4)	1.998 (6)	Pt–C(4)–Fe	79.0 (2)
Pt–P(3)	2.270(2)	Fe–Pt–C(3)	73.5 (2)
Pt–P(2)	2.319(2)	Fe–Pt–C(2)	96.2 (2)
Fe–P(1)	2.233(2)	Fe–Pt–C(1)	160.7(3)
Fe–C(4)	2.019(6)	P(1)–Fe–Pt	93.19(5)
Fe–C(3)	1.797(7)	P(2)–Pt–Fe	98.90(4)
Fe–C(2)	1.799(7)	P(3)–Pt–Fe	156.06(5)
Fe–C(1)	1.760(6)	P(2)–Pt–P(3)	104.52(5)
C(4)–C(5)	1.331(9)	C(4)–Pt–P(3)	105.6(2)
C(5)–C(6)	1.477(8)	C(4)–Pt–P(2)	149.8(2)
H–C(5)	0.73(2)	C(4)–Fe–P(1)	142.5(2)
O(1)–C(1)	1.153(8)	C(1)–Fe–C(2)	94.6(3)
O(2)–C(2)	1.142(9)	C(3)–Fe–C(2)	165.5(3)
O(3)–C(3)	1.139(8)	C(3)–Fe–C(1)	93.3(3)
P(1)–C(24)	1.845(5)	P(1)–C(24)–P(2)	111.4(3)
P(2)–C(24)	1.848(6)	C(4)–C(5)–C(6)	131.6(6)
		C(5)–C(4)–Pt	140.5(5)
		C(5)–C(4)–Fe	140.7(5)

this type.^{6,32–35} The iron and platinum atoms are linked by a dppm bridge forming a five-membered ring which has an envelope conformation, with the P(1)–C(24)–P(3) plane forming an angle of 153(3)° with the Fe–P(1)–P(2)–Pt mean plane. The bridging vinylidene ligand is symmetrically situated between the metals, with Fe–C(4) and Pt–C(4) distances of 2.019(6) and 1.998(6) Å, respectively. The same symmetric arrangement has been encountered for $[(\text{OC})_3\text{Fe}\{\mu\text{-C}(\text{Et})\text{OSi}(\text{OMe})_3\}(\mu\text{-dppm})\text{Pt}(\text{PPh}_3)]$.² The angle between the Fe–P(1)–P(2)–Pt and Fe–C(4)–Pt planes amounts to 173.9°. The length of the C(4)–C(5) double bond of 1.331(9) Å is similar to that reported for other bimetallic phenylethenylidene-bridged systems. Distances of 1.35(2), 1.329(11), 1.318(7), and 1.33(3) Å are found in $[(\text{OC})_2\text{CpMn}\{\mu\text{-C}=\text{C}(\text{H})\text{Ph}\}\text{Mn}(\text{Cp})_2]$,³⁶ $[(\text{OC})\text{Rh}(\mu\text{-dppm})_2\{\mu\text{-C}=\text{C}(\text{H})\text{Ph}\}\text{Rh}(\text{CO})_2]$,³⁷ $[(\text{OC})(\text{PCy}_3)\text{Rh}(\mu\text{-OOC-CH}_3)\{\mu\text{-C}=\text{C}(\text{H})\text{Ph}\}\text{Rh}(\text{PCy}_3)(\text{CO})][\text{BF}_4]$,³⁸ and $[\text{Pt}_2(\text{C}\equiv\text{CPh})\{\mu\text{-C}=\text{C}(\text{H})\text{Ph}\}(\text{PEt}_3)_4][\text{BF}_4]$,³⁹ respectively. The C(4)–C(5)–C(6) angle is 131.6(6)°, with the phenyl ring orientated toward the iron center. The coordination about the Fe atom is completed by three terminal CO ligands and may be viewed as distorted octahedral and that of the Pt atom as distorted square planar. The terminal PPh_3 ligand makes an angle of 156.04(4)° with the Fe–Pt bond. The overall geometry of complexes **7** is therefore similar to that of the μ -siloxycarbene $[(\text{OC})_3\text{Fe}\{\mu\text{-C}(\text{R})\text{OSi}(\text{OMe})_3\}(\mu\text{-dppm})\text{Pt}(\text{PR}_3)]$ **2**² and the μ -aminocarbene complexes $[(\text{CO})_3\text{Fe}\{\mu\text{-CNR}'\}(\mu\text{-Ph}_2\text{-PXPPH}_2)\text{Pt}(\text{PPh}_3)][\text{BF}_4]$ (X = CH₂, NH).³⁴ Crystal structure determinations performed on the latter complexes show that the sterically less demanding group R' is always oriented for steric reasons toward the platinum center.³⁵ The same orientation has been suggested for

(32) Fontaine, X. L. R.; Jacobsen, G. B.; Shaw, B. L.; Thornton-Pett, M. *J. Chem. Soc., Dalton Trans.* **1988**, 1185.

(33) Fontaine, X. L. R.; Jacobsen, G. B.; Shaw, B. L.; Thornton-Pett, M. *J. Chem. Soc., Dalton Trans.* **1988**, 741.

(34) Knorr, M.; Faure, T.; Braunstein, P. *J. Organomet. Chem.* **1993**, 447, C4.

(35) Knorr, M.; Strohm, C. Manuscript in preparation.

(36) Nesmeyanov, A. N.; Aleksandrov, G. G.; Antonova, A. B.; Anisimov, K. N.; Kolobova, N. E.; Struchkov, Y. T. *J. Organomet. Chem.* **1976**, 110, C36.

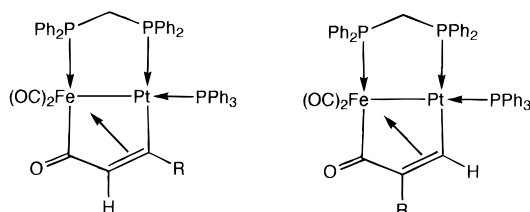
(37) (a) Berry, D. H.; Eisenberg, R. *Organometallics* **1987**, 6, 1796. (b) for a phenylethenylidene-bridged Ir–Ir complex see: Xiao, J.; Cowie, M. *Organometallics* **1993**, 12, 463.

(38) Esteruelas, M. A.; Lahoz, F. J.; Onate, E.; Oro, L. A.; Rodriguez, L. *Organometallics* **1993**, 12, 4219.

(39) Afzal, D.; Lenhart, P. G.; Lukehart, C. M. *J. Am. Chem. Soc.* **1984**, 106, 3050.

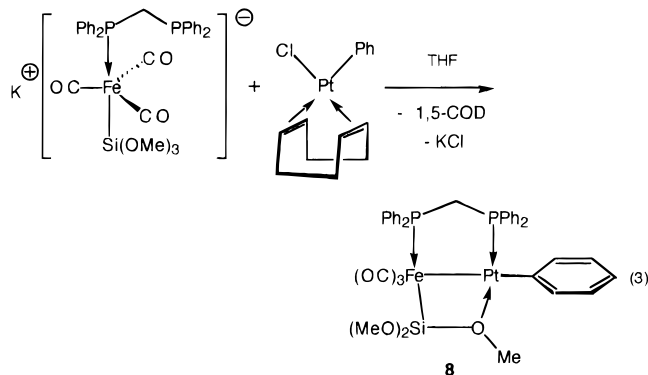
$[(OC)_2CpMn\{\mu-C=C(H)Ph\}Pt(PR_3)_2]^{23}$ and for $[(OC)-CpFe(\mu-CO)\{\mu-C=C(H)Ph\}Pt(PEt_3)_2][PF_6]^{24}$. For compounds **6**, however, the relative orientation of the bridging vinylidene ligand cannot be predicted with certainty.

It is interesting to note that two other isomeric forms of **7a** containing a five-membered metallacyclopentone bridge have been obtained by Shaw *et al.* upon treatment of $[(CO)_3Fe(\mu-CO)(\mu-dppm)Pt(PPh_3)]$ with $RC\equiv CH$ ($R = Ph, p\text{-tolyl}$).³³

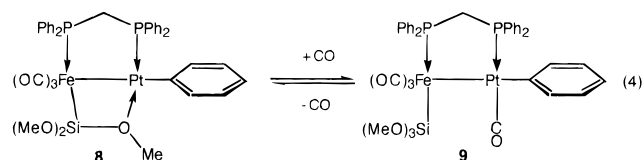


The transformation of coordinated 1-alkynes (in some cases via hydrido-alkynyl intermediates) offers meanwhile a well elaborated synthetic access for the preparation of mononuclear vinylidene complexes.^{40–45,53} Occasionally, addition of $PhC\equiv CH$ to homodinuclear complexes may lead to μ -vinylidene complexes depending on the reaction conditions.³⁷ Aspects of this 1,2 hydrogen shift have been examined theoretically.⁴⁶ The activation of phenylacetylene in heterobimetallic systems giving μ -hydrido-alkynyl compounds is also known. One example is the cationic Rh–Pt complex $[(C_5Me_5)(PMe_3)Rh\{\mu-\eta^2:\eta^1-PhC\equiv C\}(\mu-H)Pt(PPh_3)_2][OSO_2CF_3]_2$ reported by Stang and Cao.⁴⁷ The reversible interconversion between a hydrido-alkynyl and a $\mu_4-\eta^2$ -vinylidene group in a tetranuclear cluster has also been reported.^{48a} Similar species may also be intermediates during the transformation of **1a** to **6**. Until very recently,⁴⁹ this method has however not been applied to the preparation of heterobimetallic μ -vinylidene complexes. The most common methods for the preparation of heterobimetallic μ -vinylidene complexes are the addition of a second metal fragment to a mononuclear vinylidene complex^{22,23,25,43,45,49–54} or the addition of Pt–H bonds across the $C\equiv C$ bonds of transition metal alkynyl complexes.²⁴

Preparation of Fe–Pt–Ph Complexes. With the aim of extending our investigations on insertion reactions of heterobimetallic alkyl complexes to aryl-substituted heterobimetallics, we prepared the phenyl complex $[(OC)_3Fe\{\mu-Si(OMe)_2(OMe)\}(\mu-dppm)Pt(Ph)]$ **8** in 85% yield by reaction of the metalate $trans-[Fe\{Si(OMe)_3\}(CO)_3(\eta^1-dppm)]^-$ with $[PtCl(Ph)(1,5-COD)]^{55}$ in THF according eq 3.



The spectroscopic data of **8** (see Experimental Section) are very similar to those for the analogous methyl derivative and diagnostic for a rigid μ -Si–O bridge on the NMR time scale. However, this μ -Si–O bridge readily opens upon purging a CH_2Cl_2 solution of **8** with CO to give the adduct $[(OC)_3\{Si(OMe)_3\}Fe(\mu-dppm)Pt(CO)(Ph)]$ **9**, which loses in a reversible manner the CO ligand under reduced pressure.



The $^{31}P\{^1H\}$ NMR spectrum of complex **9** shows two doublets at δ 61.1 ($^{2+3}J(Pt-P) = 30$ Hz) and 16.4 ($^1J(Pt-P) = 3343$ Hz) with a $^{2+3}J(P-P)$ value of 78 Hz, which is much larger than in complexes containing a $\eta^2-\mu_2$ -Si–O bridge (see **4**). Apart from the additional absorption at 2087 cm^{-1} for the CO ligand on platinum the position for the three meridional carbonyls on iron ($1960, 1897$ and $1867, \text{ cm}^{-1}$) remains nearly unchanged. Surprisingly, no subsequent migratory insertion occurred despite the favorable mutual cis-position of the CO and phenyl groups. Even after stirring for 16 h in CH_2Cl_2 under an CO atmosphere, IR monitoring revealed no evidence for the formation of an aryl species. This contrasts with our findings that in the case of the alkyl analogues of **8** insertion has been completed quantitatively after ca. 10 min for the ethyl derivative and ca. 1 h for the methyl and norbornyl derivatives.

In a very recent study, Chen *et al.* examined the carbonylation of $trans-[Pt\{C(O)R\}(R')(PPh_3)_2]$ to yield $cis-[Pt\{C(O)R\}\{C(O)R'\}(PPh_3)_2]$ and established for the reaction rate the order $R' = Et \gg Ph > Me$.¹¹ The same tendency toward R migration in square-planar platinum complexes has also been mentioned in a review by Anderson and Cross.⁵⁶ Note, however, that for the

(40) Antonova, A. B.; Kolobova, N. E.; Petrovskii, P. V.; Lokshin, B. V.; Obezyuk, N. S. *J. Organomet. Chem.* **1977**, *137*, 55.

(41) Kolobova, N. E.; Antonova, A. B.; Khitrova, O. M.; Antipin, M. Y.; Struchkov, Y. T. *J. Organomet. Chem.* **1977**, *137*, 69.

(42) Wolf, J.; Werner, H.; Serhadli, O.; Ziegler, M. L. *Angew. Chem. Int. Ed. Engl.* **1983**, *22*, 414.

(43) (a) Werner, H. *Angew. Chem.* **1990**, *102*, 1109; *Angew. Chem., Int. Ed. Engl.* **1990**, *29*, 1077. (b) Werner, H. *Nachr. Chem. Tech. Lab.* **1992**, *40*, 435.

(44) (a) Werner, H.; Baum, M.; Schneider, D.; Windmüller, B. *Organometallics* **1994**, *13*, 1089. (b) Werner, H.; Höhn, A.; Schulz, M. *J. Chem. Soc., Dalton Trans.* **1991**, 777.

(45) Werner, H. *J. Organomet. Chem.* **1994**, *475*, 45.

(46) Silvestre, J.; Hoffmann, R. *Helv. Chim. Acta* **1985**, *68*, 1461.

(47) Stang, P. J.; Cao, D. *Organometallics* **1993**, *12*, 996.

(48) (a) Ewing, P.; Farrugia, L. *J. Organometallics* **1989**, *8*, 1246.

(b) For further examples of vinylidene-bridged clusters, see: Albiez, T.; Bernhardt, W.; v. Schnering, C.; Roland, E.; Bantel, H.; Vahrenkamp, H. *Chem. Ber.* **1987**, *120*, 141. (c) Albiez, T.; Powell, A. K.; Vahrenkamp, H. *Chem. Ber.* **1989**, *123*, 667.

(49) Wang, L. S.; Cowie, M. *Organometallics* **1995**, *14*, 2374.

(50) Kolobova, N. E.; Ivanov, L. L.; Zhvanko, O. S.; Aleksandrov, G. G.; Struchkov, Y. T. *J. Organomet. Chem.* **1982**, *228*, 265.

(51) Werner, H.; Alonso, F. J. G.; Otto, H.; Peters, K.; von Schnering, H. G. *J. Organomet. Chem.* **1985**, *289*, C5.

(52) Werner, H.; Wolf, J.; Müller, G.; Krüger, C. *J. Organomet. Chem.* **1988**, *342*, 381.

(53) Bruce, M. I. *Chem. Rev.* **1991**, *91*, 197.

(54) Schneider, D.; Werner, H. *Organometallics* **1993**, *12*, 4420.

(55) Eaborn, C.; Odell, K. J.; Pidcock, A. *J. Chem. Soc., Dalton Trans.* **1978**, 357.

(56) Anderson, G. K.; Cross, R. J. *Acc. Chem. Res.* **1984**, *17*, 67.

carbonylation of mononuclear phenylplatinum complexes containing bidentate ligands, several days are sometimes required.^{57a} The heterodinuclear complex [PtCl(Ph)(μ -Ph₂PC₅H₄)₂ZrCl₂] undergoes a smooth carbonylation within 3 days to the corresponding benzoyl complex [PtCl{C(O)Ph}(μ -Ph₂PC₅H₄)₂ZrCl₂].^{57b} We do not rule out that very slow CO insertion would occur in our system in the course of several days. The detection of an aroyl species is however complicated by the slow transformation of [(OC)₃Fe{ μ -Si(OMe)₂(OMe)}(μ -dppm)-Pt(Ph)] into [(OC)₃Fe{ μ -Si(OMe)₂(OMe)}(μ -dppm)PtCl] using chlorinated solvents. Future studies will show whether CO insertion into the Pt–Ph bond is possible under pressure.

Conclusion

These studies have shown that interesting and sometimes unpredictable bimetallic reactivity patterns may be observed. The metal–ligand interplay and the metallosite selectivity observed in these systems provide the potential for further investigations concerning (i) the insertion of small molecules into the M–C bond of our bimetallic systems and (ii) the activation of C–H bonds of 1-alkynes leading to μ -vinylidene complexes. The latter complexes are closely related to recently described μ -siloxycarbene and μ -isonitrile complexes.^{1,2,13,33} Our new results extend previous reactivity studies on cationic Si(OMe)₃ substituted Fe–Pt complexes toward alkynols HC≡CCCH₂CH(R)OH giving complexes bearing terminal carbene ligands on platinum.¹³ They are furthermore promising objects for future mechanistic and reactivity studies. We are currently investigating the reactivity of **6** and **7** toward electrophiles and testing the possibility to prepare vinylidene-bridged Fe–Pd complexes using [(OC)₃Fe{ μ -Si(OMe)₂(OMe)}(μ -dppm)-Pd{C(O)Me}] **1b** as precursor.

Experimental Section

All reactions were performed in Schlenk-tube flasks under purified nitrogen. Solvents were dried and distilled under nitrogen before use, tetrahydrofuran over sodium benzophenone-ketyl, toluene and hexane over sodium, dichloromethane from P₄O₁₀. Nitrogen was passed through BASF R3-11 catalyst and molecular sieve columns to remove residual oxygen or water. Elemental C, H, and N analyses were performed on a Leco Elemental Analyser CHN 900, FAB[–] mass spectra were obtained on a Fisons ZAB-HF spectrometer. Infrared spectra were recorded in the 4000–400 cm^{–1} region on a Perkin-Elmer 883 spectrometer. The ¹H, ³¹P{¹H}, ²⁹Si-INEPT, and ¹³C{¹H} NMR spectra were recorded at 200.13, 81.01, 39.76, and 50.32 MHz, respectively, on a Bruker ACP 200 instrument. Phosphorus chemical shifts were referenced to 85% H₃PO₄ in H₂O with downfield shifts reported as positive. ¹⁹⁵Pt chemical shifts were measured on a Bruker ACP 200 instrument (42.95 MHz) and externally referenced to K₂PtCl₄ in water with downfield chemical shifts reported as positive. NMR spectra were recorded in pure CDCl₃, unless otherwise stated. The presence of CH₂Cl₂ of solvation in **3b**, **4**, and **7** has been determined from the ¹H NMR spectrum. The reactions were generally monitored by IR spectroscopy in the ν (CO) region. 2,6-xylylisonitrile, *tert*-butylisonitrile, phenylacetylene, 1-hexyne and *tert*-butylacetylene were obtained

from Fluka and Aldrich and used as received. ¹³C-labeled **1a** and *trans*-[Fe{Si(OMe)₃(CO)₃(η ¹-dppm)][–] was prepared as described previously.⁵⁸

[(OC)₃(MeO)₃Si]Fe(μ -dppm)Pt{C(O)Me}(*t*-BuNC) (**3a**). *t*-BuNC (0.046 g, 0.55 mmol) was added to a solution of **1a** (0.423 g, 0.5 mmol) in 10 mL of CH₂Cl₂. After being stirred for 10 min, the solution was concentrated, the product precipitated by addition of hexane, and the resulting yellow powder was dried *in vacuo*. Yield: (0.464 g, 96%). Suitable yellow crystals of **3a** for the X-ray determination were grown by layering a concentrated CH₂Cl₂ solution with hexane. (Anal. Found: C, 47.07, H, 4.35; N, 1.38. Calcd for C₃₈H₄₃FeNO₇P₂PtSi (*M* = 966.72): C, 47.21, H, 4.48; N, 1.45). IR (CH₂Cl₂) ν (CN): 2205 s ν (CO): 1957 s, 1888 s, 1860 vs, 1650 m, br cm^{–1}. NMR: ¹H (298 K), δ 1.56 (s, 9H, *t*-Bu), 1.65 (s, 3H, C(O)CH₃), 3.66 (s, 9H, OCH₃), 3.89 (t, 2H, PCH₂P, ²J(P–H) = 10.6, ³J(Pt–H) = 42.4 Hz), 7.05–7.68 (m, 20H, phenyl); ³¹P{¹H}, δ 64.8 (d, P¹(Fe), ²⁺³J(P¹–P²) = 83 Hz, ²⁺³J(P–Pt) not observed), 11.1 (d, P²(Pt), ¹J(P–Pt) = 3628 Hz).

[(OC)₃(MeO)₃Si]Fe(μ -dppm)Pt{C(O)Me}(2,6-xylylNC) (**3b**). Solid xylyl-isonitrile (0.013 g, 0.10 mmol) was added to a solution of **1a** (0.084 g, 0.10 mmol) in 5 mL of CH₂Cl₂. After being stirred for 10 min, the solution was layered with hexane (ca. 10 mL) and stored at 5 °C in a refrigerator. Yellow crystals of **3b** were formed, which were collected after 2 d and dried *in vacuo*. Yield: (0.072 g, 68%) (Anal. Found: C, 48.28, H, 4.20; N, 1.33. Calc for C₄₂H₄₃FeNO₇P₂PtSi·0.5CH₂Cl₂ (*M* = 1014.77 + 42.46): C, 48.78, H, 4.47; N, 1.40). IR (CH₂Cl₂) ν (CN): 2176 s ν (CO): 1953 s, 1885 s, 1858 vs, 1649 m, br cm^{–1}. NMR: ¹H (298 K), δ 1.66 (s, 3H, C(O)CH₃), 2.47 (s, 6H, xylyl-CH₃), 3.49 (s, 9H, OCH₃), 3.87 (t, 2H, PCH₂P, ²J(P–H) = 10.6, ³J(Pt–H) = 42.4 Hz), 6.99–7.68 (m, 23H, aromatic); ³¹P{¹H}, δ 64.8 (d, P¹(Fe), ²⁺³J(P¹–P²) = 84 Hz, ²J(P–Pt) not observed), 11.1 (d, P²(Pt), ¹J(P–Pt) = 3595 Hz); ¹⁹⁵Pt{¹H}, δ –2211 (d, br, ¹J(Pt–P) = 3595 Hz); ¹³C{¹H}, δ 225.1 (d, Pt(C=O)CH₃, ²J(C–P) = 4), 215.1 (d, 2 FeCO, ²J(C–P) = 6 Hz), 213.0 (d, 1 FeCO, ²J(C–P) = 16 Hz), 135.8–126.9 (aromatic C), 50.3 (s, SiOMe), 45.3 (d, (C=O)CH₃, ³J(C–P) = 4 Hz), 41.4 (dd, PCP, ¹J(C–P) = 14, ¹J(C–P') = 34 Hz), 18.6 (s, xylyl-CH₃); ²⁹Si-INEPT, δ 13.15 (dd, ²J(Si–P) = 28, ³J(Si–P) = 4, ²J(Si–Pt) = 26 Hz).

[(OC)₃Fe{ μ -Si(OMe)₂(OMe)}(μ -dppm)Pt{(MeO₂C)C=C(CO₂Me)C(O)Me}] (**4**). DMAD (0.078 g, 0.55 mmol) was added to a solution of **1a** (0.423 g, 0.50 mmol) in 10 mL of CH₂Cl₂. After being stirred for 1.5 h, the solution was concentrated, the product precipitated by addition of hexane, and the resulting yellow powder dried *in vacuo*. Yield: (0.416 g, 78%). (Anal. Found: C, 44.38, H, 3.73. Calc for C₃₉H₄₀FeO₁₁P₂PtSi·0.5CH₂Cl₂ (*M* = 1025.70 + 42.46): C, 44.42, H, 3.87). IR (KBr) ν (CO): 1980 m, 1916 s, 1894 s, 1722s, 1678 m cm^{–1}. NMR: ¹H (293 K), δ 1.97 (s, 3H, C(O)CH₃), 3.44 (s, OMe), 3.52 (s, 3H, OMe), 3.60 (PCH₂P, partially obscured by the methoxy signals), 3.78 (s, 6H, SiOCH₃), 3.83 (s, 3H, SiOCH₃), 7.20–7.85 (m, 20H, phenyl); ³¹P{¹H}, δ 55.3 (d, P¹(Fe), ²⁺³J(P¹–P²) = 44 Hz, ²J(P–Pt) = 43 Hz), 2.1 (d, P²(Pt), ¹J(P–Pt) = 4812 Hz); ¹⁹⁵Pt{¹H}, δ –2224 (dd, ¹J(Pt–P) = 4812, ²⁺³J(Pt–P) = 44 Hz).

[(OC)₃(MeO)₃Si]Fe(μ -dppm)Pt{(MeO₂C)C=C(CO₂Me)C(O)Me}(*t*-BuNC) (**5a**). *t*-BuNC (0.009 g, 0.11 mmol) was added to a solution of **4** (0.107 g, 0.1 mmol) in 5 mL of CH₂Cl₂. After being stirred for 10 min the solution was concentrated, the product precipitated by addition of hexane, and the resulting yellow powder dried *in vacuo*. Yield: (0.102 g, 92%). (Anal. Found: C, 47.27, H, 4.25; N, 1.30. Calcd for C₄₄H₄₉FeNO₁₁P₂PtSi (*M* = 1108.84): C, 47.66, H, 4.45; N, 1.26). FAB[–] MS: 1107 (4%) [M – H][–]; IR (KBr) ν (CN): 2214 s ν (CO): 1962 s, 1896 s, 1872 vs, 1698 s, br, 1655 sh cm^{–1}. NMR: ¹H, δ 1.47 (s, 9H, *t*-Bu), 2.09 (s, 3H, C(O)CH₃), 3.23 (s,

(57) (a) Anderson, G. K.; Lumetta, G. J. *Organometallics* **1985**, *4*, 1542. (b) Anderson, G. K.; Lin, M. *Organometallics* **1988**, *7*, 2285.

(58) Braunstein, P.; Knorr, M.; Schubert, U.; Lanfranchi, M.; Tiripicchio, A. *J. Chem. Soc., Dalton Trans.* **1991**, 1507.

3H, OCH₃), 3.47 (s, 3H, OCH₃), 3.58 (s, 9H, SiOCH₃), 3.74 (m, 1H^A, PCH₂P, H^B is obscured by the SiOMe₃ resonance), 6.95–7.70 (m, 20H, phenyl); ¹³C{¹H}, δ 215.5 (s, br, 1 FeCO, ²J(C–P) not resolved), 212.8 (s, br, 2 FeCO, ²J(C–P) not resolved), 199.9 (s, (C=O)CH₃), 171.7 (s, C(O)OCH₃), 169.7 (d, PtC=C, ²J(C–P) = 7), 166.9 (s, C(O)OCH₃), 138.2 (d, PtC=C, ³J(C–P) = 7), 139.3–127.6 (aromatic C), 57.6 (s, C-CH₃), 57.6 (s, C(O)OCH₃), 52.6 (s, C(O)OCH₃), 51.3 (s, SiOMe), 40.1 (dd, PCP, ¹J(C–P) = 17, ¹J(C–P) = 34 Hz), 29.6 (s, (C=O)CH₃), 29.0 (s, *t*-Bu-CH₃); ³¹P{¹H}, δ 59.0 (d, P¹(Fe), ²⁺³J(P¹–P²) = 81 Hz, ²⁺³J(P–Pt) = 51 Hz), 11.3 (d, P²(Pt), ¹J(P–Pt) = 3146 Hz); ²⁹Si-INEPT, δ 10.80 (dd, ²J(Si–P) = 30, ³J(Si–P) = 5 Hz).

[(OC)₃(MeO)₃Si]Fe(μ-dppm)Pt{(MeO)₂C=C(CO₂Me)-(2,6-xylyl)NC} (5b). XylylNC (0.013 g, 0.1 mmol) was added to a solution of **4** (0.107 g, 0.1 mmol) in 5 mL of CH₂Cl₂. After being stirred for 10 min, the solution was concentrated, the product precipitated by addition of hexane, and the resulting yellow powder dried *in vacuo*. Yield: (0.103 g, 89%). (Anal. Found: C, 47.27, H, 4.25; N, 1.30. Calc for C₄₈H₄₉FeNO₁₁P₂PtSi (*M* = 1156.88): C, 49.83, H, 4.227; N, 1.21). FAB-MS: 1156 (8%) [M – H][–]; IR (KBr) ν(CN): 2183 s ν(CO): 1962 s, 1898 s, 1876 vs, 1700 s, br, 1660 sh cm^{–1}. NMR: ¹H, δ 2.10 (s, 3H, C(O)CH₃), 2.42 (s, 6H, xylyl-CH₃), 3.23 (s, 3H, COCH₃), 3.45 (s, 3H, COCH₃), 3.51 (s, 9H, SiOCH₃), 3.73 (m, 1H^A, PCH₂P, H^B is obscured by the SiOMe₃ resonance), 6.92–7.79 (m, 23H, aromatic); ³¹P{¹H}, δ 59.0 (d, P¹(Fe), ²⁺³J(P¹–P²) = 82, ²⁺³J(P–Pt) = 50 Hz), 12.3 (d, P²(Pt), ¹J(P–Pt) = 3138 Hz); ¹⁹⁵Pt{¹H}, δ –2583 (d, br, ¹J(Pt–P) = 3140 Hz); ²⁹Si-INEPT, δ 10.77 (dd, ²J(Si–P) = 30, ³J(Si–P) = 5 Hz).

[(OC)₃Fe{μ-C=C(H)Ph}(μ-dppm)Pt(CO)] (6a). To a solution of **1a** (0.423 g, 0.50 mmol) in 5 mL of CH₂Cl₂ was added a tenfold excess of phenylacetylene. After being stirred for 24 h, the solution was concentrated, and the product precipitated by addition of hexane. The resulting oily residue was dried *in vacuo* for 1 h and then extracted with warm Et₂O. After slow concentration a brownish powder precipitated, which was filtered off and dried *in vacuo*. Yield: (0.251 g, 59%). A second extraction of the crude material (ca. 95% purity by ³¹P NMR) with warm Et₂O afforded the analytically pure product. (Anal. Found: C, 52.69, H, 3.72. Calc for C₃₇H₂₈FeO₄P₂Pt (*M* = 849.50): C, 52.31, H, 3.32). IR (CH₂Cl₂) ν(CO): 2021 m, 2011 s, 1953 vs, ν(C=C): 1591 w cm^{–1}. NMR: ¹H, δ 4.17 (t, 2H, PCH₂P, ²J(P–H) = 10.2, ³J(Pt–H) = 41.6 Hz), 6.77–7.75 (m, 25H, phenyl), 8.65 (dd, 1H, vinylidene, ⁴J(P–H) = 9.5, 18.3 Hz); ¹³C{¹H} (253 K), δ 238.5 (dd, α-C, ²J(P–C) = 11, 58), 215.9 (s, br, FeCO), 212.6 (d, 2 FeCO, ²J(P–C) = 16 Hz), 188.7 (s, br, Pt–CO), 143.9 (s, br, β-C, ²J(Pt–C) = 114 Hz), 46.7 (t, PCP, ¹J(P–C) = 26 Hz); ³¹P{¹H}, δ 60.8 (d, P¹(Fe), ²⁺³J(P¹–P²) = 125, ²⁺³J(P–Pt) = 80), 21.9 (d, P²(Pt), ¹J(P–Pt) = 2368 Hz); ¹⁹⁵Pt{¹H}, δ –2336 (dd, ¹J(Pt–P) = 2367, ²⁺³J(Pt–P) = 80 Hz).

[(OC)₃Fe{μ-C=C(H)*t*-Bu}(μ-dppm)Pt(CO)] (6b). To a solution of **1a** (0.423 g, 0.50 mmol) in 5 mL of CH₂Cl₂ was added a fivefold excess of *tert*-butylacetylene. After stirring for 5 h, the solution was concentrated, and the product precipitated by addition of hexane. The resulting oily residue was dried *in vacuo* for 1 h and then redissolved in a CH₂Cl₂/hexane mixture. After slow concentration an orange powder precipitated, which was filtered off and dried *in vacuo*. Yield: (0.282 g, 68%). (Anal. Found: C, 50.35, H, 4.29. Calc for C₃₅H₃₂FeO₄P₂Pt (*M* = 829.51): C, 50.68, H, 3.89). IR (KBr) ν(CO): 2020 m, 2005 s, 1951 vs, 1927 sh, ν(C=C): 1584 w cm^{–1}. NMR: ¹H, δ 1.29 (s, 9H, *t*-Bu), 4.16 (t, 2H, PCH₂P, ²J(P–H) = 10.2, ³J(Pt–H) = 40.9), 7.12–7.67 (m, 20H, phenyl), 7.83 (dd, 1H, vinylidene, ⁴J(P–H) = 11.0, 19.0, ³J(Pt–H) = 24.6); ¹³C{¹H} (295 K), δ 228.1 (dd, α-C, ²J(P–C) = 11, 59), 216.7 (s, br, FeCO), 213.4 (d, 2 FeCO, ²J(P–C) = 15), 189.1 (s, br, PtCO), 155.4 (s, br, β-C, ²J(Pt–C) = 112), 128.2–137.3 (phenyl), 47.5 (t, PCP, ¹J(P–C) = 27, ²J(Pt–C) = 89) 35.1 (dd, C-CH₃, ⁴J(P–C) = 3, 13), 30.8 (s, *t*-Bu-CH₃), (253 K), δ 228.1 (dd, α-C, ²J(P–C) = 11, 59 Hz), 216.6 (d, FeCO, ²J(P–C) = 3),

213.2 (d, 2 FeCO, ²J(P–C) = 15), 188.7 (t, PtCO, ²J(P–C) ≈ ³J(P–C) = 5 Hz), 155.0 (s, br, β-C, ²J(Pt–C) = 112); ³¹P{¹H}, δ 61.2 (d, P¹(Fe), ²⁺³J(P¹–P²) = 131, ²⁺³J(P–Pt) = 76 Hz), 22.6 (d, P²(Pt), ¹J(P–Pt) = 2355 Hz); ¹⁹⁵Pt{¹H}, δ –2326 (dd, ¹J(Pt–P) = 2356, ²⁺³J(Pt–P) = 76 Hz).

[(OC)₃Fe{μ-C=C(H)*n*-Bu}(μ-dppm)Pt(CO)] (6c). This complex has only been characterized spectroscopically. ³¹P{¹H}, δ 61.4 (d, P¹(Fe), ²⁺³J(P¹–P²) = 128, ²J(P–Pt) = 80 Hz), 22.9 (d, P²(Pt), ¹J(P–Pt) = 2374 Hz); ¹⁹⁵Pt{¹H}, δ –2375 (dd, ¹J(Pt–P) = 2374, ²J(Pt–P) = 80 Hz).

[(OC)₃Fe{μ-C=C(H)Ph}(μ-dppm)Pt(PPh₃)] (7a). To a CH₂Cl₂ solution of **6a**, prepared *in situ* from **1a** (0.50 mmol) and PhC≡CH, was added PPh₃ (0.5 mmol, 0.131 g). After stirring for 1 h, the red-brown solution was concentrated to ca. 5 mL and layered with hexane. Yellow-orange crystals were formed, which were collected after storage for 1 d at ambient temperature and two further days at 5 °C. Yield: (0.349 g, 62%) (Anal. Found: C, 58.12; H, 4.17. Calc for C₅₄H₄₃FeO₃P₃Pt·0.5CH₂Cl₂ (*M* = 1083.79 + 42.46): C, 58.12; H, 3.94). IR (KBr) ν(CO): 1988 m, 1922 vs, 1911 sh, ν(C=C): 1580 w cm^{–1}; NMR: ¹H, δ 3.99 (dt, 2H, PCH₂P, ²J(P–H) = 10.0, ⁴J(P–H) = 1.5, ³J(Pt–H) = 37.5 Hz), 6.32 (ddd, 1H, vinylidene, ⁴J(P–H) = 2.4, 6.0, 34.6 Hz), 6.83–7.78 (m, 40H, C₆H₅); ³¹P{¹H}, δ 63.4 (dd, P¹(Fe), ²⁺³J(P¹–P²) = 116, ³J(P¹–P³) = 14, ²J(P–Pt) = 79 Hz), 43.3 (dd, P³(Pt), ²J(P²–P³) = 18, ³J(P¹–P³) = 14, ¹J(P–Pt) = 4022 Hz), 21.9 (dd, P²(Pt), ¹J(P–Pt) = 2472 Hz); ¹³C{¹H} (253 K), δ 236.9 (dd, α-C, ²J(P–C) = 10, 70 Hz), 218.2 (d, FeCO, ²J(P–C) = 10), 215.3 (dd, 2 FeCO, ²J(P–C) = 16, ³J(P–C) = 4 Hz), 141.1 (s, br β-C, ²J(Pt–C) = 110 Hz), 52.3 (dt, PCP, ¹J(P–C) = 15, 19 Hz); ¹⁹⁵Pt{¹H} (CH₂Cl₂/CDCl₃), δ –2695 (ddd, ¹J(Pt–P) = 4022, 2473, ²⁺³J(Pt–P) = 79 Hz).

[(OC)₃Fe{μ-C=C(H)*t*-Bu}(μ-dppm)Pt(PPh₃)] (7b). To a CH₂Cl₂ solution of **6b**, prepared *in situ* from **1a** (0.5 mmol) and *t*-BuC≡CH, was added PPh₃ (0.5 mmol, 0.131 g). After stirring for 2 h, the red-brown solution was concentrated to ca. 5 mL, and the yellow product was precipitated by slow addition of hexane. Yield of the spectroscopically nearly pure product: (0.420 g, 79%). Analytically pure yellow-orange crystals were grown from CH₂Cl₂/hexane. (Anal. Found: C, 57.32; H, 4.75. Calc for C₅₂H₄₇FeO₃P₃Pt·0.5CH₂Cl₂ (*M* = 1063.80 + 42.46): C, 57.01; H, 4.38). IR (KBr) ν(CO): 1986 m, 1919 vs, 1909 sh, ν(C=C): 1581 w cm^{–1}; NMR: ¹H (CDCl₃), δ 0.98 (s, 9H, *t*-Bu), 3.98 (dt, 2H, PCH₂P, ²J(P–H) = 9.8, ⁴J(P–H) = 1.8, ³J(Pt–H) = 38.4 Hz), 6.43 (ddd, 1H, vinylidene, ⁴J(P–H) = 6.4, 11.2, 27.8 Hz), 7.01–7.40 (m, 35H, C₆H₅); ¹³C{¹H} (295 K), δ 223.0 (dd, α-C, ²J(P–C) = 10, 71), 218.9 (s, br, FeCO), 216.5 (unresolved, 2 FeCO), 153.1 (s, br, β-C, ²J(Pt–C) = 110), 53.0 (dt, PCP, ¹J(P–C) = 15, 19), 34.5 (d, C-CH₃, ⁴J(P–C) = 13), 30.5 (s, *t*-Bu-CH₃); ³¹P{¹H}, δ 63.5 (dd, P¹(Fe), ²⁺³J(P¹–P²) = 122, ³J(P¹–P³) = 15, ²J(P–Pt) = 78 Hz), 44.3 (dd, P³(Pt), ²J(P²–P³) = 22, ³J(P¹–P³) = 15, ¹J(P–Pt) = 4072 Hz), 22.4 (dd, P²(Pt), ¹J(P–Pt) = 2490 Hz); ¹⁹⁵Pt{¹H} (CH₂Cl₂/CDCl₃) δ –2715 (ddd, ¹J(Pt–P) = 4072, 2490, ²⁺³J(Pt–P) = 78 Hz).

[(OC)₃Fe{μ-C=C(H)*t*-Bu}(μ-dppm)Pt{P(OMe)₃}] (7c). To a solution of **6b** (0.2 mmol, 0.166 g) in CH₂Cl₂ (3 mL) was added P(OMe)₃ (0.25 mmol, 0.031 g). After stirring for 15 min (CO evolution), all volatiles were removed under *vacuo*. The oily residue was triturated with hexane (ca. 4 mL) and dried again to give an orange-yellow powder. Yield: (0.181 g, 90%) (Anal. Found: C, 45.34; H, 4.86. Calc for C₃₇H₄₁FeO₆P₃Pt·CH₂Cl₂ (*M* = 925.58 + 84.93): C, 45.17; H, 4.29). IR (KBr) ν(CO): 1991 m, 1924 vs, 1914 sh, ν(C=C): 1584 w cm^{–1}; NMR: ¹H δ 1.33 (s, 9H, *t*-Bu), 3.45 (d, 9H, POME, ³J(P–H) = 13.1), 4.16 (dt, 2H, PCH₂P, ²J(P–H) = 10.0, ⁴J(P–H) = 2.2, ³J(Pt–H) = 35.3), 7.15–7.85 (m, 21H, C₆H₅ and obscured vinylidene proton); ¹³C{¹H} (295 K), α-C and FeCO not detected, 152.6 (s, β-C, ²J(Pt–C) = 122), 127.9–138.6 (m, phenyl), 51.2 (s, POCH₃, ²J(P–C) = 18), 51.0 (m, PCP, partially obscured), 34.7 (d, CCH₃, ⁴J(P–C) = 13 Hz), 30.8 (s, *t*-Bu-CH₃); ³¹P{¹H} δ 153.6 (dd, P³(Pt), ²J(P²–P³) = 14, ³J(P¹–P³) = 23, ¹J(P–Pt) = 6479 Hz), 63.8 (dd, P¹(Fe), ²⁺³J(P¹–P²) = 125,

Table 3. Summary of Crystallographic Data, Intensity Measurements, and Refinement for 3a and 7a·0.5CH₂Cl₂

	3a	7a·0.5CH₂Cl₂
empirical formula	C ₃₈ H ₄₃ FeNO ₇ P ₂ PtSi	C _{54.5} H ₄₄ ClFeO ₃ P ₃ Pt
fw	966.70	1126.20
T, K	293(2)	293(2)
λ(Mo Kα), pm	71.073	71.073
cryst syst	monoclinic	triclinic
space group	<i>P</i> 2 ₁ / <i>n</i>	<i>P</i> 1
a, pm	1108(2)	1238.8(2)
b, pm	1866.5(13)	1311.4(2)
c, pm	2022(2)	1631.5(2)
α, deg	90	107.260(9)
β, deg	99.71(9)	93.790(9)
γ, deg	90	103.420(9)
V, pm ³	4.124(7)	2.4359(5)
Z	4	2
d(calcd), g/cm ³	1.557	1.535
abs coeff, mm	3.893	3.362
F(000)	1928	1122
cryst size, mm	0.95 × 0.40 × 0.35	0.25 × 0.25 × 0.32
diffractometer	Siemens Stoe AED 2	Stoe IPDS
θ-range, deg	1.97 to 24.01	2.31 to 24.16
index ranges (−h/h, −k/k, −l/l)	−12/12, 0/21, 0/23	−13/12, −15/14, −18/18
no. of reflns colled	6448	15683
no. of indep reflns	6448	7228
no. of obs reflns [I > 2σ(I)]	4995	7083
no. of restraints/params	0/467	0/590
goodness of fit	1.039	1.065
R(F) [I > 2σ(I)]	0.0415	0.0381
Rw(F) ² all data	0.1157	0.1101
largest diff peak/hol, e pm ^{−3}	171	110

³J(P¹–P³) = 23, ²J(P–Pt) = 71 Hz), 22.3 (dd, P²(Pt), ¹J(P–Pt) = 2286 Hz); ¹⁹⁵Pt{¹H}, δ –2686 (ddd, ¹J(Pt–P) = 6479, 2286, ²⁺³J(Pt–P) = 71 Hz).

[(OC)₃Fe{μ-C=C(H)*t*-Bu}(μ-dppm)Pt(C≡N-xylyl)] (7d).

To a solution of **6b** (0.083 g, 0.10 mmol) in CH₂Cl₂ (5 mL) was added solid 2,6-xylyl isonitrile (0.015 g, 0.11 mmol). After the solution was stirred for 10 min, the solvent was removed *in vacuo*. The residue was then triturated with hexane (ca. 4 mL) and dried again to give an orange-yellow powder. Yield: (0.082 g, 88%) (Anal. Found: C, 53.48, H, 4.72, N, 1.30. Calcd for C₄₃H₄₁FeNO₃P₂Pt·0.5CH₂Cl₂ (*M* = 932.68 + 42.46): C, 53.58, H, 4.34, N, 1.43). IR (CH₂Cl₂) ν(CN): 2106 s ν(CO): 2005 s, 1934 vs, ν(C=C): 1584 w cm^{−1}, (KBr) ν(CN): 2103 s ν(CO): 1993 s, 1924 vs, ν(C=C): 1584 w cm^{−1}. NMR: ¹H, δ 1.30 (s, 9H, *t*-Bu), 2.10 (s, 6H, PhCH₃), 4.09 (t, 2H, PCH₂P, ²J(P–H) = 9.5, ³J(Pt–H) = 36.7 Hz), 6.91–7.71 (m, 23H, aromatic), 7.84 (dd, 1H, vinylidene, ⁴J(P–H) = 11.4, 18.1, ³J(Pt–H) = 20.6 Hz); ¹³C{¹H} (253 K), δ 226.5 (dd, α-C, ²J(P–C) = 10, 68 Hz), 217.6 (d, FeCO, ²J(P–C) = 3 Hz), 215.3 (d, 2 FeCO, ²J(P–C) = 15 Hz), 158.4 (m, br, PtCNR), 152.9 (s, br, β-C, ²J(Pt–C) = 123), 127.6–137.8 (m, phenyl), 48.9 (t, PCP, ¹J(P–C) = 27), 34.6 (dd, CCH₃, ⁴J(P–C) = 3, 13 Hz), 30.7 (s, *t*-Bu-CH₃), 18.9 (s, xylyl-CH₃); ³¹P{¹H}, δ 63.9 (d, P¹(Fe), ²⁺³J(P¹–P²) = 128, ²J(P–Pt) = 72 Hz), 19.5 (d, P²(Pt), ¹J(P–Pt) = 2363 Hz); ¹⁹⁵Pt{¹H}, δ –2376 (d, br, ¹J(Pt–P) = 2366 Hz, ²⁺³J(Pt–P) not resolved).

[(OC)₃Fe{μ-Si(OMe)₂(OMe)}(μ-dppm)Pt(Ph)] (8).

A solution of K[Fe(CO)₃{Si(OMe)₃}(η¹-dppm)] (0.380 g, 0.55 mmol) in THF (20 mL) was added to a suspension of [PtCl(Ph)(1,5-cod)] (0.50 mmol) in THF (3 mL). The reaction mixture was stirred for ca. 3 h. The resulting clear orange solution was filtered through Celite, and the solvent was removed under reduced pressure. Extraction of the residue with two portions of Et₂O (2 × 20 mL) and addition of hexane to the combined fractions led to the precipitation of **8** on reducing the volume under reduced pressure. The brown-orange product, which was air-stable for short periods of time in the solid state, was isolated in 80% yield. (Anal. Found: C, 48.64; H, 4.12. Calcd for C₃₇H₃₆FeO₆P₂PtSi (*M* = 917.65): C, 48.43; H, 3.95%). IR (THF) ν(CO): 1960 m, 1901 s, 1873 s, (CH₂Cl₂): 1960 m, 1899 s, 1867 s. NMR: ¹H, δ 3.17 (s, br, 3H, PtOCH₃, ³J(Pt–H) =

21.5 Hz), 3.59 (t, partially obscured by the Si(OMe)₃ resonance, 2H, PCH₂P, ²J(P–H) = 10.1 Hz), 3.72 (s, 6H, SiOCH₃), 6.60–7.65 (m, 25H, C₆H₅); ¹³C{¹H}, δ 217.2 (d, 2 FeCO, ²J(P–C) = 18 Hz), 212.9 (d, FeCO, ²J(P–C) = 11 Hz), 122.8–135.9 (phenyl), 54.7 (s, PtOCH₃), 50.7 (s, SiOCH₃), 44.9 (m, PCP, not resolved); ³¹P{¹H}, δ 62.1 (d, P¹(Fe), ²⁺³J(P¹–P²) = 41, ²J(P–Pt) = 65 Hz), 8.2 (d, P²(Pt), ¹J(P–Pt) = 5181 Hz); ¹⁹⁵Pt{¹H}, δ –2328 (dd, ¹J(Pt–P) = 5181, ²⁺³J(Pt–P) = 65 Hz).

X-ray Crystal Structure Determinations. Crystallographic details are given in Table 3. Suitable single crystals of **3a** and **7a·0.5CH₂Cl₂** were grown by slow diffusion of hexane into a CH₂Cl₂ solution at room temperature. Data of **3a** were collected at room temperature on a Stoe-Siemens-diffractometer using the 2θ/ω-scan type. Three standard reflections were monitored every 90 min; no significant decay was noticed over the data collection period. Intensities were corrected for Lorentz and polarization effects. Absorption corrections derived from Ψ scans of three reflections were applied. Data of **7a·0.5CH₂Cl₂** were collected at room temperature on a Stoe-IPDS-diffractometer. No significant decay was noticed over the data collection period. Intensities were corrected for Lorentz and polarization effects. The structures were solved by Patterson methods and refined first by full-matrix least-squares with isotropic thermal parameters and then by full-matrix least-squares with anisotropic thermal parameters for all non-hydrogen atoms.⁵⁹ All hydrogen atoms were placed at their geometrically calculated positions and refined "riding" on the corresponding carbon atoms, except H(5) of **7a·0.5CH₂Cl₂**, which was refined isotropic. Refinement of a disordered *tert*-butyl group for **3a** by a splitting model for C(11), C(12), and C(13) gave no significant improvement of the *R*-values. The largest remaining peaks in the final difference map were equivalent to about 1.7 e/Å^{−3} (**3a**) and 1.1 e/Å^{−3} (**7a**), respectively, and located near Pt. The scattering factor coefficients and anomalous dispersion coefficients were taken from ref 60.

(59) (a) Sheldrick, G. M. SHELXS-86, Universität Göttingen, 1986. (b) Sheldrick, G. M. SHELXL-93, Universität Göttingen, 1993.

(60) *International Tables for X-Ray Crystallography*, Kynoch Press, Birmingham, U.K., 1974; Vol. IV.

Acknowledgment. The Deutsche Forschungsgemeinschaft is gratefully thanked for habilitation grants and financial support to M. K and C. S., the CNRS (Paris) for support to the Strasbourg laboratory (P.B. and M.K.), and the DEGUSSA AG for a generous gift of Pd and Pt salts. M.K. and C.S. are also indebted to Prof. M. Veith for his support and providing institute facilities.

Supporting Information Available: Final atomic coordinates are given in Tables S1 and S2. Tables of hydrogen atom coordinates (Tables S5), thermal parameters for the non-hydrogen atoms (Tables S4), and complete lists of bond distances and angles (Table S3) (19 pages). Ordering information is given on any current masthead page.

OM9602670